The Cost of Being Big: Local Competition, Importance of Dispersal, and Experimental Evolution of Reversal to Unicellularity

María Rebolleda-Gómez[1,*] and Michael Travisano[1,2]

1. Department of Ecology, Evolution, and Behavior, University of Minnesota, Saint Paul, Minnesota 55108; and Minnesota Center for Philosophy of Science, University of Minnesota, Minneapolis, Minnesota 55455; 2. BioTechnology Institute, University of Minnesota, Saint Paul, Minnesota 55108

Submitted November 15, 2017; Accepted June 21, 2018; Electronically published October 24, 2018

Online enhancements: appendix figures. *Dryad data:* https://doi.org/10.5061/dryad.32b87rn.

ABSTRACT: Multicellularity provides multiple benefits. Nonetheless, unicellularity is ubiquitous, and there have been multiple cases of evolutionary reversal to a unicellular organization. In this article, we explore some of the costs of multicellularity as well as the possibility and dynamics of evolutionary reversals to unicellularity. We hypothesize that recently evolved multicellular organisms would face a high cost of increased competition for local resources in spatially structured environments because of larger size and increased cell densities. To test this hypothesis we conducted competition assays, computer simulations, and selection experiments using isolates of *Saccharomyces cerevisiae* that recently evolved multicellularity. In well-mixed environments, multicellular isolates had lower growth rates relative to their unicellular ancestor because of limitations of space and resource acquisition. In structured environments with localized resources, cells in both multicellular and unicellular isolates grew at a similar rate. Despite similar growth, higher local density of cells in multicellular groups led to increased competition and higher fitness costs in spatially structured environments. In structured environments all of the multicellular isolates rapidly evolved a predominantly unicellular life cycle, while in well-mixed environments reversal was more gradual. Taken together, these results suggest that a lack of dispersal, leading to higher local competition, might have been one of the main constraints in the evolution of early multicellular forms.

Keywords: multicellularity, cooperation, resource limitation, local competition, dispersal, experimental evolution.

* Corresponding author; present address: Department of Biological Sciences, University of Pittsburgh, Pittsburgh, Pennsylvania 15260; email: rebol004@umn.edu.

ORCIDs: Rebolleda-Gómez, http://orcid.org/0000-0002-3592-4479; Travisano, http://orcid.org/0000-0001-8168-0842.

Am. Nat. 2018. Vol. 192, pp. 731–744.
DOI: 10.1086/700095

Introduction

Multicellularity provides multiple benefits, including reduced predation (Stanley 1973; Maynard Smith and Szathmáry 1995) and division of labor between cells (Pfeiffer et al. 2001; Michod 2007). These benefits come with costs. Cells that defect from cooperation can potentially gain the benefits of multicellularity without the costs and thereby increase in frequency. This defection, when unchecked, leads to dissolution and death of the multicellular individual. Most research has focused on the challenges of conflict mediation among cells within an organism, as well as between individual and collective interests (Buss 1987; Sober and Wilson 1998; Pfeiffer et al. 2001; Michod 2007). However, the difficulties of cooperation are not the only constraints faced by multicellular individuals.

Multicellularity has evolved more than 20 times in eukaryotes, with substantial variation among the resulting forms (Grosberg and Strathmann 2007). Although research into these differences has largely focused on aspects of conflict mediation (e.g., Sebé-Pedrós et al. 2017), changes in the size and cellular organization associated with these evolutionary transitions provide their own challenges (Solari et al. 2006; Sommer et al. 2017). In particular, trade-offs associated with size have frequently been identified as important constraints in multicellular species (Stearns 1989), with potential consequences for fecundity and dispersal (Yu and Wilson 2001; Hanski et al. 2006). These trade-offs, their ecological context, and their evolutionary consequences remain largely unexplored in the context of the origins of multicellularity.

In multicellular microorganisms, body size can have profound effects on dispersal (Herron and Michod 2008) and resource use (Pfeiffer et al. 2001). Adaptations to these body size challenges typically involve modes of cellular specialization that facilitate, for example, dispersal of the organism (or its offspring) and the distribution of nutrients (Smith

et al. 2014). Nascent multicellular species are unlikely to have many adaptations to multicellularity given their recent evolutionary history; this includes adaptations involving trade-offs associated with the increased size of multicellular organisms. In this article, we explored the potential for these trade-offs to lead to an evolutionary reversal—from multicellularity to unicellularity—in a nascent multicellular system. We asked how ecological factors affect the maintenance of nascent multicellularity and thereby gain insight about the factors limiting transitions to multicellularity more broadly. Combining modeling and experimental evolution, we investigated the persistence of multicellularity in two environments that differ dramatically in their effects on dispersal and resource availability: surfaces (spatially structured) and well-mixed aqueous environments (mass action).

In well-mixed environments, rapid dispersal throughout the environment occurs passively. Similarly, resources and waste products are rapidly distributed throughout the environment, such that every individual has equal access to resources. In contrast, passive dispersal of microbes is strongly limited in spatially structured environments. While diffusion of resources and waste products does occur in surface environments, it is far slower than in well-mixed environments. Thus, these environments differ in the propensity to promote intercellular cooperation (Escalante et al. 2015). In well-mixed environments, cooperation can be lost because of diffusion of public goods and their benefits to noncooperating individuals (Chao and Levin 1981; Greig and Travisano 2008). In contrast, spatial structure tends to facilitate and stabilize public goods cooperation even among different bacterial species (Harcombe 2010) and promote the evolution of undifferentiated multicellularity in yeast (Koschwanez et al. 2011), and it may facilitate differentiation and increased metabolic efficiency (Pfeiffer et al. 2001; Bachmann 2013). Spatial structure provides an advantage for cooperation because the public goods benefits of cooperation tend to accrue to the individuals producing the public good (Driscoll and Pepper 2010). The effects of environmental differences on multicellularity are much less clear in the absence of public goods–mediated cooperation.

Snowflake yeast are the evolutionary outcome of a selection experiment for increased body size, initially carried out over 60 serial passages starting with unicellular *Saccharomyces cerevisiae* (Ratcliff et al. 2012). The snowflake morphology consists of a network of cells connected by incomplete cell separation, so that daughter cells remain attached to their mother cells, which in turn are attached to their progenitors. This is a mode of staying-together multicellularity (Bonner 1998; Grosberg and Strathmann 2007; Tarnita et al. 2013). These multicellular strains evolved as a response to a selection experiment favoring increases in size and are orders of magnitude larger than an individual yeast cell (Ratcliff et al. 2012; Rebolleda-Gómez et al. 2012). We hypothesized that snowflake yeast multicellularity would not be beneficial in the absence of body size selection and that the costs would differ substantially between the two environments in ways that are distinct from public goods–mediated cooperation. In snowflake yeast, the benefits of cooperation are not mediated by diffusible compounds. Rather, the benefits are restricted to the clustering of the clonal cells themselves, as the larger body size itself was beneficial in the original selection experiment. In this article, we show that the interplay between resource acquisition and dispersal plays a major role in shaping the scales of competition (local or global) and therefore the costs of staying-together multicellularity. These ecological conditions shape the dynamics of reversibility to unicellularity, prior to any conflicts associated with cooperation.

Methods

System

To evaluate the importance of dispersal, local competition, and local limitation of resources during transitions to multicellularity, we used a recently developed experimental system. Multicellular isolates of the brewer's yeast *Saccharomyces cerevisiae* evolved as a result of a selection experiment favoring larger sizes. Ratcliff et al. (2012) performed a selection experiment in which a single clone of *S. cerevisiae* Y55 was used to initiate 10 replicate populations. After 60 days of daily gravitational selection (transferring only the first fraction of culture that settles to the bottom), all of the populations evolved multicellularity. The strains used throughout this study were five multicellular isolates (from five different replicate populations) and their common unicellular ancestor (for isolation procedures, see Rebolleda-Gómez et al. 2012). All strains were grown in YPD (1% yeast extract, 2% peptone, and 2% dextrose) or YPD plates (15.5% agar). We used the ancestral unicellular strain *S. cerevisiae* Y55 and a single multicellular isolate from one of the 10 populations (C1W8.2) for the growth assays and estimation of growth parameters. This is a tractable system in which dispersal can be manipulated. In this system we can address the importance of increased size, local competition, and dispersal in the evolution of multicellularity and reversals to unicellularity.

Growth Measurements

To compare growth dynamics between unicellular and multicellular strains in a mass-action environment (with homogeneously distributed resources), we measured the changes in optical density at 600 nm (OD_{600}) of one of the multicellular isolates (C1W8.2) and the unicellular ancestor in a microplate reader (Tecan infinite 200Pro). Liquid cultures (5 μL) were placed at different concentrations of YPD (100%, 75%,

50%, 25%, 20%, 15%, 10%, and 1%) in separate wells of a 24-well plate with a total volume of 500 μL per well. Optical density was measured every 15 min for 24 h. The plate was kept at 29.9°C and shaken to keep multicellular clusters from settling (between measurements: 300 s of linear shaking with 3.5 mm of amplitude, 300 s of orbital shaking with 3.5 mm of amplitude, and 300 s of linear shaking again with 3.5 mm of amplitude). To standardize these data in terms of biomass, we also measured the optical density of multicellular and unicellular cultures in a serial dilution and then extracted and quantified the total protein content of these cultures through mechanical cell lysis and the Bradford assay. For the Bradford assay results, we used the ratio of absorbances at 595 nm over 450 nm to extend the linear range and minimize errors associated with saturation (Zor and Selinger 1996).

We performed linear regression to evaluate the relation between optical density and total protein content with phenotype (unicellular or multicellular) as a factor. We found a nonsignificant effect of phenotype (1.854 ± 1.005 SE μg) and phenotype by OD_{600} (-0.85 ± 0.562 SE $\mu g/OD_{600}$) on the relation between OD_{600} and protein content. Differences between phenotypes were mainly due to two outliers. This effect overestimates the initial densities and total differences between unicellular and multicellular phenotypes (fig. A2; figs. A1–A3 are available online). Calculating the protein concentration by phenotype leads to a large difference in initial densities, even though all cultures were initiated with approximately the same number of cells (there is a difference between mean initial concentrations using independent estimations for each phenotype [95% confidence interval (CI), 0.912 to 1], whereas there is no difference in the initial density using the same biomass standardization across phenotypes [95% CI, −0.07 to 0.014]). Thus, these differences are most likely not meaningful biological variation but differences in effective lysis of the cells. To avoid this problem, we removed phenotype from our model and used the resulting estimates of intercept and slope ($\text{TotProt} = 1.9 + 1.8\ OD_{600}$, $R^2 = 0.76$) to convert our OD_{600} data to total protein biomass in micrograms per milliliter.

Similarly, to measure growth in a spatially structured environment, we plated 20 μL of a 1:4 dilution of an overnight culture of our unicellular and multicellular strains on mini agar plates (15.5% agar) in the wells of a 24-well plate. We placed these plates in the incubator facing down on a scanner without a lid and scanned the plates every half hour for 60 h. We converted the images to 8 bit and removed the background by subtracting the initial scan from all following images and increasing the contrast. We then identified an area (the same size and shape for all wells) that contained most of the culture but avoided the light reflection of the walls of each well (fig. A1) and calculated the average pixel density over time for each of the samples. We performed all of the image analysis using ImageJ2 (Schindelin et al. 2015). We used a similar procedure for standardization (i.e., cell lysis and Bradford assay), but in this case we plated six cultures of different concentrations for each phenotype and measured their density using the same methods. We then resuspended these cultures and measured the total protein content. Again, independent estimations of biomass led to an overestimation of differences in initial density despite largely overlapping CIs (fig. A2). We used the more conservative estimates, using the simpler model (with only the effect of pixel density on protein concentration) to calculate the total protein content of our growth curve samples ($\text{TotProt} = 4.1 + 0.44\ OD_{600}$, $R^2 = 0.63$).

In this system, the rate of cell growth depends on the concentration of available resources R. The change in yeast cell density N over time can then be described with a simple system of two differential equations:

$$\frac{dN}{dt} = N\mu(R), \tag{1}$$

$$\frac{dR}{dt} = -N\frac{1}{\alpha}\mu(R), \tag{2}$$

where α is the yield (how many microbial cells are produced per microgram of resources) and $\mu(R)$ is the Monod (1949) function describing nutrient uptake efficiency depending on resource concentration:

$$\mu(R) = \frac{\mu_{\max} R}{R + K_R}. \tag{3}$$

To evaluate differences in growth between unicellular and multicellular isolates, we fitted the Monod growth model (Monod 1949) using the nls function in R (Pinheiro and Bates 2000; Pinheiro et al. 2015; R Core Team 2018) and compared the models in which the two main parameters were kept fixed or allowed to vary between strains (Ritz and Streibig 2008). We obtained the parameter estimates for the saturation constant K_R and the maximum growth rate $\mu_{\max}$ from the model, allowing for different groups, and obtained confidence regions using the R package ellipse (Murdoch and Chow 2013; growth data and parameter estimations are available in the Dryad Digital Repository: http://doi.org/10.5061/dryad.32b87rn; Rebolleda-Gómez and Travisano 2018).

Competition Assays

To estimate the cost of multicellularity in mass action (liquid) and spatially structured (agar plate) environments, we performed a series of competition assays. We grew five multicellular isolates and their unicellular ancestor (Y55) for 24 h in YPD at 30°C with constant shaking at 250 rpm. After 24 h of growth, we mixed 500 μL of each of the multicellular cultures with 500 μL of the Y55 culture. We diluted and plated a sub-

sample on a petri plate with YPD to count colony-forming units (CFUs) at the initial time point (t_0). We incubated this plate for 48 hours to allow for a clear differentiation between unicellular (small and smooth) and multicellular (big and rough) colonies. We also diluted these mix cultures in a 1:4 ratio and spot plated 20 μL on a microplate (YPD agar in wells of a 24-well plate) for a total effective dilution (TED) of 1:200. We then grew the microplates for 24 hours at 30°C, resuspended the cultures in saline solution, diluted them, and plated them again at a 1:200 TED for 2 more days. At the end of three transfers, we diluted the cultures and plated them again on a petri dish with YPD agar for 48 h to count the number of CFUs of each phenotype (unicellular vs. multicellular). Simultaneously, we performed another competition experiment starting from the same mixes but transferring 50 μL of liquid culture into 10 mL of YPD without any settling selection. We performed three independent replicates of these competition assays and calculated the relative fitness (w) of each as the ratio of the realized multicellular Malthusian parameter over the realized unicellular Malthusian parameter. The realized Malthusian parameter of each phenotype P is defined as

$$M_P = \frac{\ln[N(t_3) \cdot \mathrm{DF}/N(t_0)]}{\mathrm{days}}, \quad (4)$$

where N is the number of CFUs of phenotype P and DF is the dilution factor of all transfers combined (Lenski et al. 1991). To evaluate whether fitness in liquid was associated with the proportion of cells growing, we performed a Spearman's correlation between our approximation of the average proportion of cells growing in a multicellular isolate and the relative fitness of that isolate against its unicellular ancestor in liquid medium.

Model

To evaluate the effect of local resource competition and limited dispersal for unicellular and multicellular isolates, we used the empirical growth parameters to simulate competition in a structured environment. We started with a grid of n patches, each with the same amount of resources. From there, the algorithm of the simulations works as follows: first, the grid is populated with single cells and multicellular organisms (with an initial population of 50,000 cells in a 1:1 ratio between multicellular and unicellular cells) distributed randomly. Because multicellular clusters in the strain we used to measure growth differences have on average 146 cells, we divided the seed number of cells (i.e., 25,000) by 146 and randomly spread these individuals on the grid. We then multiplied the number of individuals in each patch by the size of a multicellular individual sampled from a truncated normal distribution with a lower limit of one cell, a mean value of 146 cells per cluster, and a standard deviation of 109 (fig. A3). We tested the effect of this variance in size on fitness, but it did not affect the mean fitness differences, only the spread of these differences across simulations (see the section "Model" in "Results").

After the initial distribution, cells grow and consume resources in each patch according to equations (1) and (2) using the mean values of the maximum growth rate $\mu_{\max}$ and the saturation constant k_R of unicellular and multicellular isolates (both phenotypes have largely overlapping 95% confidence regions). The yield value (α) and resources per patch were chosen such that populations could recover after 200-fold dilution and 24 h of growth given a total concentration of resources of ≈2,500 μg/mL. The yield value (α = 0.00035 μg/cell) was larger than the weight of a single yeast cell, accounting for the use of resources in metabolism and cell construction (Bryan et al. 2010). To allow for growth expansion within a plate, once resources in a patch are exhausted, the excess population is dispersed into the adjacent eight patches and allowed to grow according to the same rules. To deal with edges, a border with zero resources was established around our grid. This border has the net effect of limiting growth around the edges—there are fewer resources around, and a very small number of cells will not grow—reproducing the edge effects of plates. Finally, after 24 h of growth in the simulations, the number of unicellular and multicellular cells is divided by 200 (dilution event), and the procedure is repeated in a new grid with the same initial concentration of resources (fig. A3; code is available in Dryad: http://doi.org/10.5061/dryad.32b87rn; Rebolleda-Gómez and Travisano 2018).

The size of multicellular isolates was manipulated by changing the parameters of the truncated normal distribution while maintaining the mean initial number of CFUs. We also explored the effect of cell density (by modifying the number of patches) and dispersal within the plate (by allowing dispersal to adjacent cells to occur earlier—i.e., at lower population sizes relative to growth within the patch). The relative time of dispersal was calculated as the ratio between the number of doublings left in a patch (from the predefined population size at the time of the first dispersal event to the carrying capacity of a patch) and the average number of doublings in a patch (from the average initial patch size to the carrying capacity of a patch).

Selection Experiments

Finally, to evaluate the effect of dispersal costs on evolutionary reversals to unicellularity, we analyzed data from five of the populations of a larger selection experiment that looked at the dynamics of reversibility of multicellular yeast. In this experiment we propagated in batch culture each of 10 multicellular isogenic strains of *S. cerevisiae* in

three replicate plates with YPD agar. Every 24 h, we resuspended each culture in 1 mL of saline solution (0.85% NaCl). These cultures were then diluted fourfold. We then plated 20 μL of these dilutions on a new YPD plate (for a TED of 1:200). Samples from each replicate were frozen at −80°C in 20% glycerol every week. For the liquid control, we repeated the experiment with five of the initial strains (again, three replicates per strain) and transferred every day a 200-fold dilution into 1 mL of YPD.

To determine the number of unicellular individuals over time (as well as the size distributions of each culture), we regrew half of our frozen samples (all the time points of all the replicate populations of the five multicellular ancestors used for the competition experiments). We grew the strains for 24 h of conditioning in YPD. Then these cultures were diluted tenfold in saline solution, and 1 mL of each sample was run through a FlowCam instrument (Fluid Imaging Technologies) using a ×10 objective and C70 syringe. The areas of all of the clusters measured were recorded, and circularity and size filters were used to eliminate measurements of air bubbles or other particles in the medium. For the purposes of this study, we analyzed data from only five time points (0, 4, 11, 17, and 30 transfers). The proportion of single cells was calculated from the areas of the particles.

Results

Growth Dynamics and Fitness Differences

Multicellular snowflake yeast evolved in a simple environment where resources diffuse freely; all spatial structure during growth is imposed by the multicellularity itself (Libby et al. 2014). In this environment (and assuming that all cells have the same resource uptake capabilities), single cells have equal access to resources. However, the evolution of multicellularity leads to a spatial reorganization of cells. These incipient multicellular phenotypes develop through incomplete separation of mother and daughter cells and reproduce through fission facilitated by the evolution of increased rates of apoptosis. Dead cells weaken linkages, facilitating asymmetrical division of small clonal propagules (Ratcliff et al. 2012, 2015; Libby et al. 2014). In these multicellular clusters there are some cells (at the center) that—as a result of limited nutrient diffusion or lack of space—do not divide (Ratcliff et al. 2012). Multicellular isolates pay a cost in terms of growth and, in the absence of settling selection, have lower fitness than their unicellular ancestor (Ratcliff et al. 2012).

To compare growth dynamics between unicellular and multicellular strains in a mass action environment, we measured changes in biomass over time. Using equation (3), we estimated the maximal growth rate and the saturation constant: $\mu_{\max}$ is the maximum potential of growth in the absence of nutrient limitation, and K_R is the concentration of resources at which growth is half the maximum growth rate (Monod 1949; Stewart and Levin 1973). Differences in growth between multicellular and unicellular isolates can be reflected in either or both of these parameters, depending on the mechanisms of limitation. The maximal growth rate ($\mu_{\max}$) will be lowered if, at a high concentration of resources, there are still cells growing (and consuming resources) but at a slower rate (limited by space and diffusion of nutrients). The saturation constant (K_R) will be higher if, at a low concentration of resources, there are fewer cells growing and actively converting resources into cell material (Monod 1949).

We found significant differences between the two phenotypes ($F_{2,46} = 76.97$, $p < .00001$). These differences were amplified when using independent estimates of biomass for unicellular and multicellular phenotypes (see "Methods"; fig. A2). Unicellular isolates had a higher maximal growth rate ($\mu_{\max} = 0.441 \pm 0.017$ SE for unicellular vs. $\mu_{\max} = 0.39 \pm 0.026$ SE for multicellular) and reached half of their maximal growth rate at approximately half of the total resource concentration ($K_R = 8{,}011 \pm 952$ SE for unicellular vs. $K_R = 16{,}037 \pm 2{,}593$ SE for multicellular). From these growth estimations we can conclude that the growth of multicellular isolates is limited in liquid medium relative to their unicellular ancestor (fig. 1), resulting in a net cost in relative fitness when grown in competition (fig. 2).

To illustrate these results, assume that these multicellular individuals are spherical and that only an external layer of cells is growing. We can then calculate the volume growing (V_g) for each cluster i as

$$V_{gi} = \begin{cases} \frac{4\pi}{3}(\rho_i^3 - (\rho_i - nr)^3) & \rho_i > nr, \\ \frac{4\pi}{3}\rho_i^3 & \rho_i \le nr, \end{cases} \tag{5}$$

where ρ_i is the radius of the cluster i, r is the radius of a cell, and n is the depth of the growing outer layer in number of cells. With small values of n, the proportion of growing cells rapidly decreases. The internal volume of a cluster increases much more rapidly than the external layer. Therefore, in populations of single cells and small clusters where $nr \ge \rho_i$ all cells are growing, but as the size of clusters increases this proportion drops.

Assuming a constant distribution of sizes for each isolate and spherical multicellular clusters, we calculated the proportion of biomass growing for five different populations ($n = 3$ cells, $r = 2.5$ μm). Differences in mean sizes (and thus proportion of cells growing) are consistent with differences in the relative fitness of multicellular isolates against their unicellular ancestor (fig. 2). This model is a simplification of growth to facilitate comparison between this mass action environment and a spatially structured one. How-

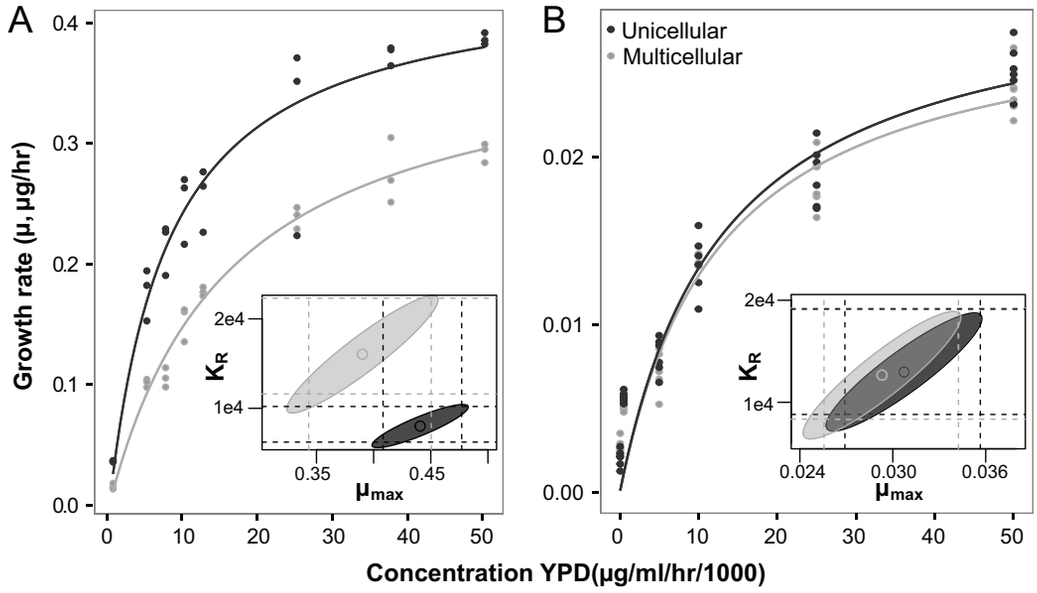

Figure 1: Resource-dependent growth of multicellular (gray) and unicellular (black) isolates on liquid medium (*A*) and on agar plates (*B*). Points are the estimated growth rates from empirical growth curves, and lines are the fitted Monod equation for each strain. Insets show estimates of the maximum growth rate μ_{max} and the saturation constant K_R with their respective 95% confidence regions. Dashed lines indicate the 95% univariate confidence intervals.

ever, consistent with the work of Ratcliff et al. (2012), it highlights the importance of small propagules as a way to compensate for the growth costs of large individuals. For example, the multicellular isolate from population 3 has some of the largest clusters, but on average its size is smaller because of a large fraction of very small propagules; thus, it has an overall larger proportion of growing cells. The isolate from population 2, in contrast, has smaller adult clusters but a much narrower distribution (Rebolleda-Gómez et al. 2012).

In a structured environment, like a solid agar plate with medium, dynamics are different. In this environment, given that single cells cannot disperse after cell division, dynamics of growth and resource uptake are expected to be similar to those of cells in a multicellular cluster. To test this prediction, we evaluated growth of the unicellular ancestor and one of the derived multicellular phenotypes (the same strains we used to evaluate differences of growth in liquid medium) on agar plates at high densities. As expected and in contrast to our results in liquid medium, when grown on plates unicellular and multicellular isolates display the same dynamics of resource-dependent growth. The estimated parameters of the maximum growth rate (unicellular, $\mu_{max} = 0.033 \pm 0.002$ SE; multicellular, $\mu_{max} = 0.031 \pm 0.002$ SE) and saturation constant (unicellular, $K_R = 12{,}464 \pm 2{,}404$ SE; multicellular, $K_R = 12{,}120 \pm 2{,}224$ SE) are similar for multicellular and unicellular isolates (fig. 1). As a result, the null hypothesis of these parameters being equal cannot be rejected when comparing models with or without an effect of phenotype ($F_{2,67} = 0.4748, p = .6241$). Using independent estimations of biomass (for multicellular and unicellular isolates) led to larger differences in growth dynamics, with a smaller estimate of multicellular maximum growth rate ($\mu_{max} = 0.026 \pm 0.002$ SE) but still overlapping confidence regions of K_R (see "Methods"; fig. A2). Overall, our results suggest that growth on spatially structured environments reduces the differences between multicellular and unicellular phenotypes.

To measure the costs of multicellularity in terms of fitness, we grew five of these multicellular isolates—each in competition with its unicellular ancestor—in two different environments: liquid medium with constant agitation (mass action) and agar plates (spatially structured). In the mass action environment, fitness of multicellular isolates was lower than that of their unicellular ancestor, indicating that multicellular individuals paid a cost in terms of growth (a reduction of ≈10% relative to their unicellular ancestor; fig. 2). In structured environments, despite having similar growth dynamics, unicellular strains rapidly took over—fitness costs of multicellular strains were consistently greater in this environment (≈20% reduction relative to the unicellular ancestor; fig. 2).

Model

This puzzling result—unicellular strains outcompeting multicellular isolates in spatially structured environments despite similar growth dynamics—can be explained by taking into ac-

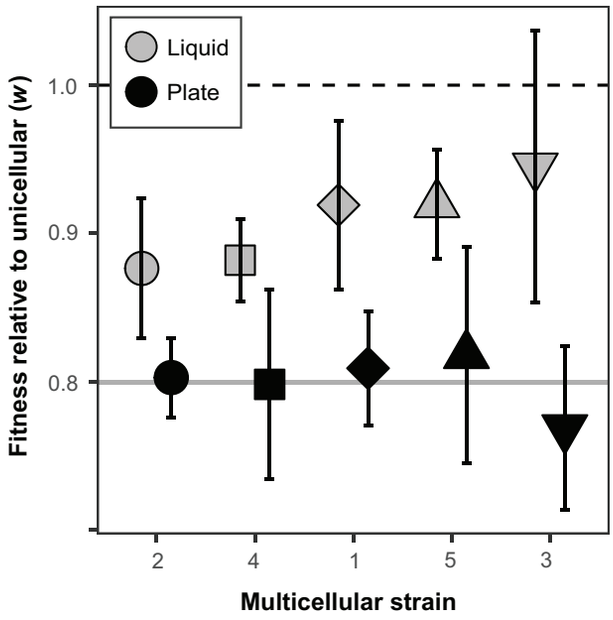

Figure 2: Relative fitness of five multicellular isolates (represented by different symbols) in competition against their unicellular ancestor. Competitions were realized in liquid medium (gray) and on plates (black). Data points are mean values ($n = 3$), and error bars represent 95% confidence intervals. The mean fitness cost from 200 simulations is denoted by the gray solid line. The multicellular strains are ordered according to the proportion of cells growing B_g (assuming perfect spheres and that an external layer three cells thick is the only part actively growing), showing a monotonic association with their relative fitness in liquid medium ($\rho_S = 1, p = .017$).

count the local dynamics of competition and local resource availability. In the spatially structured environment, resources are locally distributed; therefore, the effects of neighboring density (due to limited dispersal) and local competition are important for the overall dynamics. To evaluate the consequences of dispersal and local competition in our plate experiments, we developed spatially explicit simulations from our growth data and models. These simulations are a useful heuristic to understand the results and allow us to explore the relative importance of different parameters for the relative fitness costs of multicellular isolates.

We started with a grid of n patches, each with the same amount of resources, then distributed unicellular and multicellular isolates across the grid (same number of cells per group) and allowed them to grow using the parameters obtained from our growth assays. To avoid differences due to growth rate, we used mean values (unicellular and multicellular isolates together) of the growth rate $\mu_{\max}$ and the saturation constant k_R (these values have highly overlapping 95% confidence regions; fig. 1). In this model, after 24 h of growth, cells were diluted and redistributed across the grid (see "Methods"; fig. A3).

In this structured environment, differences in growth between unicellular and multicelluar isolates are shaped by local competition and the initial distribution of cells (i.e., the initial density of cells in each location). Given that single cells and multicellular clusters have the same growth dynamics, differences in fitness depend on the cluster's ability to disperse and secure local resources. Large multicellular clusters can rapidly outcompete their unicellular counterparts within a patch because they start with a larger population size and rapidly secure resources. At the plate scale, however, unicellular cells are better distributed across the plate (fig. 3) and therefore are able to access more resources per cell and increase their population size at a faster rate. Additionally, each dispersal event allows single cells to expand their access to nutrients and thus increase their fitness advantage (fig. 3).

This dispersal advantage of unicellular isolates is consistent with the results from our competition experiments. The CIs of our empirical fitness costs all overlap with the CIs of our simulations. However, our simulations were based on the sizes of one of our populations (population 1) and fail to capture some of the variation from isolates of different sizes (e.g., population 3 isolates have some of the largest individual clusters, and their fitness cost is higher than those of the other isolates; fig. 2).

As multicellular clusters increase in size, cells in a patch become more crowded, increasing local competition. Thus, the fitness of multicellular phenotypes (in competition with single cells) decreases very rapidly as the average size of clusters increases. As multicellular clusters get even larger, however, the rate of fitness decline decreases. Most cells of multicellular individuals at this point are distributed in only a few patches, and their growth is rapidly slowed down. As a result, adding more cells to a patch makes less of a difference, and the increasing size of clusters has a smaller effect on growth. The spread of sizes (variance) has a minimal effect on the overall fitness cost and affects only the spread of outcomes (fig. 4).

Similar to the effect of size, changes in overall cell density affect the intensity of local competition and thus the relative fitness costs of multicellularity. As density increases (i.e., there are more cells per patch), single cells are more likely to end up crowded in a few patches. This increase in density results in stronger local competition and reduces the difference between multicellular and unicellular isolates. In the opposite direction, as density decreases, the relative costs of multicellularity increase, until virtually all individuals start alone in their own patch and costs can no longer increase (fig. 4).

Local dynamics within a patch are influenced by movement between patches. In these simulations, we can modify dispersal by changing the number of individuals in a patch by the time of the first dispersal event to adjacent patches (roughly, how quickly colonies spread relative to their growth).

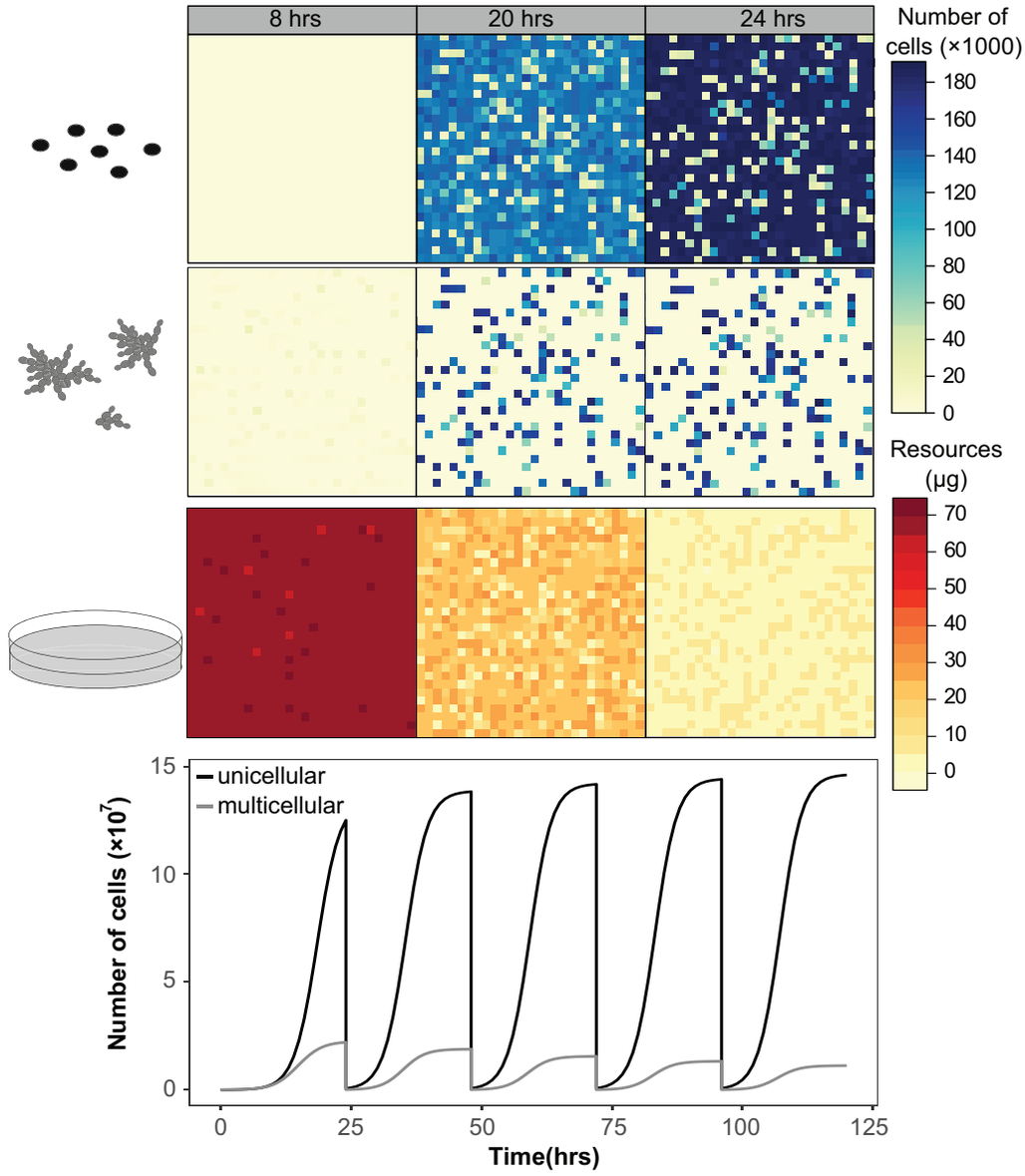

Figure 3: Simulation of competition in a spatially structured environment. The top six panels (yellow to blue) show cell densities of multicellular and unicellular strains at different time points (8, 20, and 24 h) during the first growth cycle, while the lower three panels (yellow to red) show the concentration of resources at the same time intervals. The graph shows the total number of cells over time for multicellular (gray) and unicellular (black) strains. Unicellular strains increase in frequency with each dilution and dispersal event.

Consistent with our previous results, under slow dispersal multicellular isolates pay a large cost in terms of fitness, and this cost rapidly increases with the size of the cluster. As dispersal increases, the costs of multicellularity decrease, and so do the differences among sizes. Large multicellular isolates are able to secure local resources and more rapidly expand into adjacent patches, compensating for their initial heterogeneous distribution within the plate. The results of these simulations highlight the importance of dispersal and local competition for fitness in spatially structured environments and demonstrate how these factors can severely limit multicellularity.

Selection Experiments

Fitness costs associated with increased local competition in spatially structured environments have long-term evo-

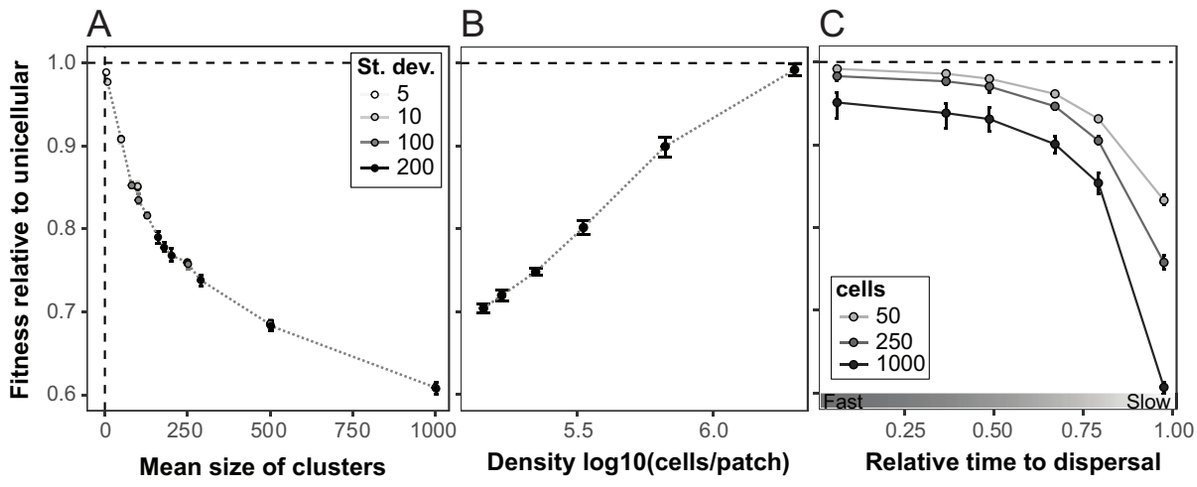

Figure 4: Effect of different parameters on our simulated fitness costs. The *Y*-axis is always the relative fitness of the multicellular phenotype against the unicellular one. *A*, Impact of the distribution of multicellular sizes (*X*-axis is the mean sizes, and the different shades of gray indicate varying degrees of dispersion in standard deviations). *B*, Effect of the density (cells/patch) on $\log_{10}$ scale. *C*, Role of dispersal (fast or slow relative to growth) on the relative fitness of clusters of different sizes (gray scale). Points represent the mean, and the error bars show the 95% confidence intervals after six simulations.

lutionary consequences for multicellular isolates. We performed selection in both mass action and spatially structured environments. Initially, our populations started with only multicellular individuals with a fraction (10%–30%) of one to three cell propagules that later develop into larger adults. In the spatially structured environment, after only 4 days of selection, most replicate lines of all ancestral populations had a majority of single cells. After 17 days of the experiment, most lines were dominated by functionally single cells (fig. 5). Moreover, and in contrast to the initial single-cell propagules, single cells isolated after 17 transfers would not develop into multicellular individuals but stayed unicellular throughout.

In the structured environment, differences in growth alone are insufficient to explain fitness differences and the rapid evolutionary reversal to single cells. Localized interactions and the dispersal and distribution of cells and resources play an important role in shaping the evolutionary dynamics. In contrast to our treatment lines, lines from our control experiment (transferred in liquid without settling selection between transfers) changed very little in the first 14 days, and after 30 days of evolution they were still mostly multicellular (fig. 5). Despite differences in growth between unicellular and multicellular strains being stronger in this mass action environment, observed reversibility consisted of a more gradual decrease in size and single cells remained infrequent throughout the experiment (fig. 5).

These results are consistent with our theoretical expectations: in liquid and in the absence of settling, there is selection for a reduction in size, but the strength of selection rapidly decreases with smaller cluster volumes until all cells in a cluster are growing at the same rate (at which point growth is equivalent to that of single cells). In spatially structured environments, multicellular isolates face great fitness costs over a larger range of sizes, and unicellularity (or near unicellularity) is strongly favored. However, even in spatially structured environments the cost of size rapidly decreases, and the fitness differences between unicellular and very small multicellular phenotypes become minimal (fig. 4). Small multicellular isolates (<405 μm^2 of area) are able to persist for more than 30 days in our selection experiment.

We calculated the time it would take for single cells to reach fixation in the presence of only these small multicellular isolates, using a continuous model of haploid selection (Lenski et al. 1991):

$$\frac{dP}{dt} = r_{\text{uni}} P(1 - P). \tag{6}$$

Our yeast strains are diploid, but because we are looking at only two discrete phenotypes and evolution proceeds without sex, we can use P and $1 - P$ as the phenotypic frequencies. Starting with 50% of each phenotype ($P = 0.5$) and with the selection rate value obtained from our simulations ($r_{\text{uni}} = 0.07$, in competition with multicellular isolates that small), we can calculate the time to fixation of single cells. This gives us an estimate of the time to fixation of 240 generations, or ≈35 transfers.

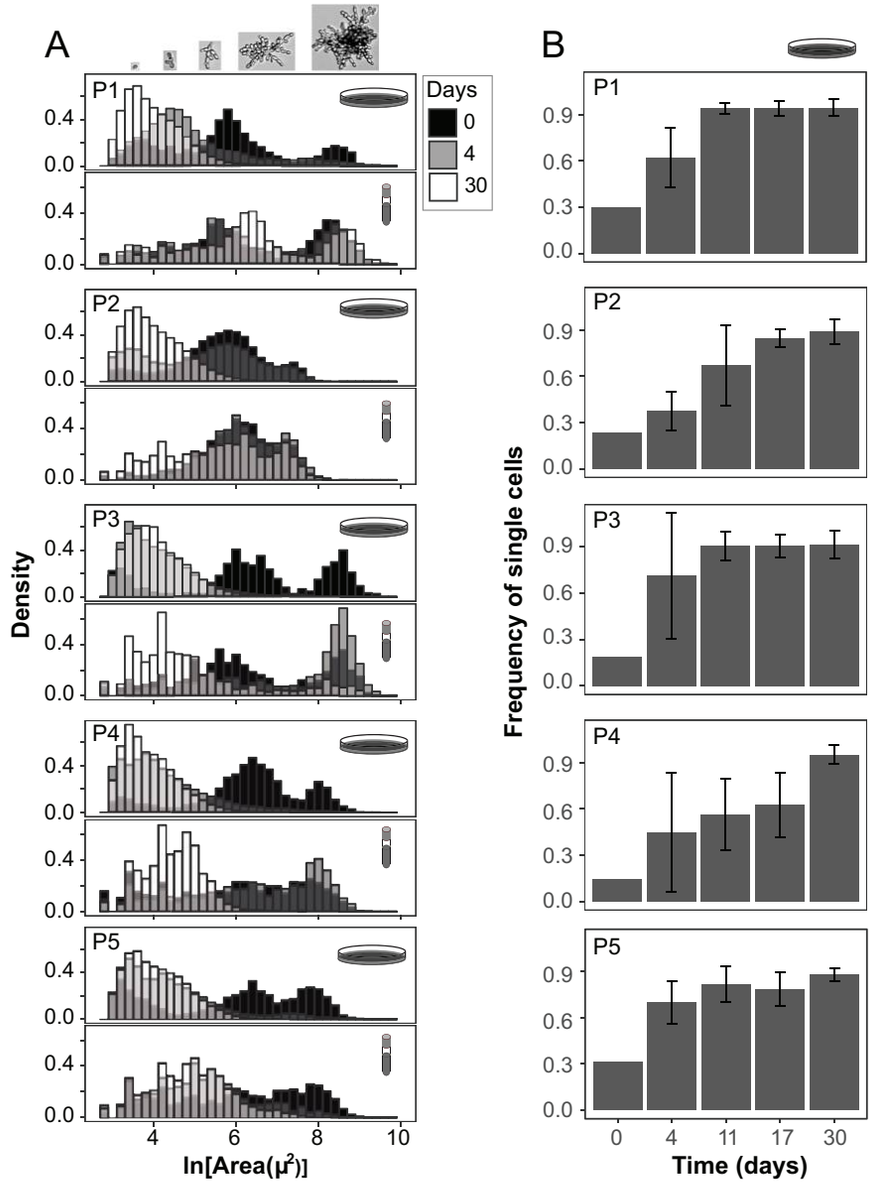

Figure 5: Dynamics of reversibility to single cells. *A*, Histogram of sizes after 0, 14, or 30 transfers on spatially structured (*upper graph*) or mass action (*lower graph*) environments. Each panel of two graphs shows data from lines derived from different ancestral strains (P1–P5). Pictures at the top exemplify the different cluster sizes. *B*, Frequency of functionally single cells over time. Each panel shows data obtained from three replicate lines derived from each of the five ancestral populations. Error bars represent 95% confidence intervals.

Taken together, these results emphasize the importance of size and resource acquisition in limiting the evolution of multicellularity and favoring rapid reversals to unicellularity. In mass action environments, multicellular organisms pay a high cost of growth due to limited space and resource diffusion. In structured environments (despite similar growth constraints for unicellular and multicellular isolates), multicellular isolates face increased local competition and pay a higher relative fitness cost in competition with their unicellular ancestor. Both growth limitation in a mass action environment and increased local competition in structured environments act as strong selective pressures favoring a rapid reduction in size. In mass action environments this reduction is gradual, leading after 30 days to a population of mainly small multicellular isolates. In structured environments, all replicate populations reverted to mostly single cells and very small multicellular isolates that persist due to small fitness differences.

Discussion

The history of life is marked by events of rapid evolution and increased complexity. Many of these transitions involve the integration of units previously capable of growth and reproduction of their own into a larger individual: independent replicators into chromosomes, prokaryotic cells into the complex and compartmentalized eukaryotic cells, single cells into multicellular organisms, and different organisms into complex societies (Maynard Smith and Szathmáry 1995; West et al. 2015). It has been proposed that the first step in these evolutionary transitions is the evolution of cooperative groups (West et al. 2015). But while cooperation and alignment of fitness are required for multicellularity, the emphasis on cooperation can obscure the importance of other ecological drivers and limits to multicellularity (e.g., dispersal and demographic structure).

Early multicellular organisms represented a dramatic increase in size from their unicellular ancestors (Payne et al. 2009). The evolution of multicellular complexity requires large numbers of cells and high degrees of cooperation (Bell and Mooers 1997). But an increase in size also restricts dispersal and nutrient uptake (Solari et al. 2006; Sommer et al. 2017). Our results underscore one of the main costs of increased size and group living (namely, increased intragroup competition), as well as the importance of dispersal in the evolution of large, cooperative groups. Theoretical work has shown that the cost of increased competition within a group can cancel out the benefits of cooperation (even among close relatives) in conditions of limited dispersal (Taylor 1992; Wilson et al. 1992; Queller 1994). These models expand Hamilton's rule to account for competition between relatives. They show that in viscous populations (i.e., a population with minimal dispersal), even though cooperation is favored by the high relatedness between individuals in a patch, the benefits of cooperation are matched by the costs of competition between kin (Taylor 1992; Queller 1994; West et al. 2002). Instead, if cooperation remains local (where cooperative individuals disproportionately benefit each other) and competition occurs at a larger scale (avoiding the relative increased cost for cooperative genotypes), then cooperative traits should be favored (Platt and Bever 2009). These results contrast with studies focusing on diffusible public goods, demonstrating the importance of ecological mechanisms in determining evolutionary outcomes (Saxer et al. 2009).

In this system, despite the costs of increased size, competition for resources occurs primarily at a global scale in liquid cultures. Resources are evenly distributed across the environment with most cells having equal access, especially in smaller individuals, where all cells have the same potential for resource use and growth. Even in large clusters, a large proportion of biomass is actively growing. Additionally, clonal staying-together multicellularity increases the spatial assortment of genotypes (increasing the probability of interaction with a closely related cell; Ratcliff et al. 2015). In these conditions, cooperation can be favored, and competition within a group is minimized. The advantages of group formation and cooperation do not need to be very large to outweigh the costs (Platt and Bever 2009). Multiple observations are consistent with these conclusions: multicellularity readily evolves in this environment (Ratcliff et al. 2012), cooperative traits like secretion of a catalytic enzyme (invertase) can favor the evolution of multicellular phenotypes (Koschwanez et al. 2011), and snowflake yeast phenotypes do not easily revert back to unicellularity even in the absence of settling selection (fig. 5).

In structured environments, our results suggest that the formation of large multicellular groups increases local competition and limits access to nutrients. These conditions of high local competition between kin are detrimental for the evolution of cooperation (Taylor 1992; Wilson et al. 1992; Queller 1994; Platt and Bever 2009). The evolution of cooperation is required for decoupling of group and individual fitness, which allows for the evolution of multicellular organisms even at the cost of cellular growth and reproduction (Michod and Roze 2001; Okasha 2005). Mass action environments pose costs for cellular growth in multicellular individuals, but competition remains mostly global, and genotypic assortment does not result in more intensified local competition. In spatially structured environments and in the absence of efficient dispersal mechanisms of the group as a whole, nascent staying-together multicellularity faces large costs of increased local competition. These dispersal constraints are likely to have played an important role as barriers for multicellular life to colonize land. Animals had to evolve complex mechanisms of motility before they could leave the aquatic environment; the early evolution of land plants involved key innovations for dispersal and increased spore protection (Graham 1993), and many (if not all) of the terrestrial origins of multicellularity are primarily dispersal structures that developed through cells coming together. These multicellular organisms can easily transition between unicellular and multicellular lifestyles (e.g., fruiting bodies of dictyostelids and myxobacteria; Bonner 1998).

Our models and experiments are simplifications of the potential conditions faced by early multicellular forms. One of the main limitations of our simulations is that they do not explicitly include diffusion of nutrients. Explicit descriptions of resource diffusion have been shown to be important in describing interactions of microbial cells in spatially structured environments (e.g., Mitri et al. 2011; Harcombe et al. 2014). In our simulations, each patch is defined by its carrying capacity and can be thought of as the area at which diffusion of resources has a significant effect on cell growth. In our simulations, this simplification is not as significant because the effect of resource diffusion on microbial growth rapidly decreases with distance (Vulin et al. 2014; Chacón

et al. 2018), and all our simulations were performed at high cell densities with microbes growing and consuming resources at a faster rate than diffusion outside immediately adjacent areas (patches). An additional limitation is that both our simulations and our experimental system depend on periodic serial transfer events imposed by the researcher. These periodic dilutions can be thought of as a temporally varying environment and alternation between growth and dispersal events, but the importance of these processes during transitions to multicellularity remains to be seen. Despite these limitations, all of our results (i.e., computer simulations, competition assays, and selection experiments) are consistent with increased costs of local competition associated with the evolution of multicellular phenotypes.

In this experiment, the costs of multicellularity in spatially structured environments were enough to rapidly select for reversals to unicellularity, with the exception of long-term persistence of very small multicellular isolates. Reversals on plates took ≈2 weeks for all of our populations, and the change was mostly discrete (from multicellular to unicellular phenotypes). In contrast, as a result of transfers in liquid without settling selection, multicellular strains showed a more continuous reduction in size (fig. 5). And in similar experiments (with the same selection pressures and strains) after 160 days of selection, multicellular phenotypes were still dominant (W. C. Ratcliff, personal communication). Our competition results suggest that a large fraction of small propagules can effectively reduce the costs of growth in mass action environments. However, these propagules are insufficient to compensate for the large costs of big groups in spatially structured environments. As a result, only very small multicellular isolates persisted after 1 month of selection in spatially structured environments.

Rapid and frequent reversals to unicellularity (as seen in this experiment) are more likely to occur in earlier stages during transitions to multicellularity. As multicellular organisms evolve more integration and reduced conflict between cells, reversals are likely to be less common. Moreover, as multicellular organisms adapt, they accumulate mutations that might be neutral or beneficial for cells in a multicellular organism but come with a cost for free-living cells. Similarly, integration of multicellular organisms is often associated with traits that might increase fitness of the multicellular individual as a whole but are costly in terms of cell-level fitness. The accumulation of these mutations can rapidly ratchet cells into a group life cycle, constraining the potential of reversibility to unicellularity (Libby and Ratcliff 2014). During these evolutionary transitions, ecological processes are likely to interact with the genetic architecture of cells, shaping the ease, stability, limits, and potential evolutionary consequences of these transitions. Future work should address the importance of genotype-by-environment interactions in the evolution of these qualitatively novel phenotypes.

This article contributes to our understanding of the processes and selective pressures relevant for transitions in individuality. Substantial prior research has identified defection and diffusible public goods as key factors affecting the propensity for the evolutionary origins of multicellularity (Michod 2007) and its persistence (Strassmann et al. 2000; Velicer et al. 2000). One of the key insights from these studies is that unequal acquisition of the benefits conferred by multicellularity can lead to dissolution of multicellular cooperation. In this article, we show that while such circumstances are sufficient for multicellular cooperation to collapse, they are not necessary. The fitness costs of multicellularity can lead to its rapid loss, with more rapid and complete dissolution occurring with greater fitness costs. Increased recognition of the breadth of circumstances that can affect multicellular persistence provides insight into the evolutionary consequences of its benefits. In particular, we note the diversity of organisms that are not neatly classifiable into unicellular or multicellular forms—often coming together at different parts of the life cycle and then dispersing as single cells—and suggest that ecological context may play a key role in the apparent plasticity in multicellular cooperation.

Acknowledgments

We thank Allison Shaw and everyone at the University of Minnesota biological theory group for advice on simulations. Emilie Snell-Rood, Ruth Shaw, Vaughn Cooper, Ford Denison, Jake Grossman, Amy Kendig, Melanie Bowman, and two reviewers all provided useful feedback and thoughtful comments. We especially acknowledge all the feedback provided by editors Judith L. Bronstein and Ben M. Bolker. This work was developed as part of M.R.-G.'s doctoral dissertation with support from the Interdisciplinary Center for the Study of Global Change as well as the Interdisciplinary Doctoral Fellowship and Doctoral Dissertation Fellowship from the graduate school at the University of Minnesota. We thank Will Harcombe for the use of his plate reader and thoughtful discussions. M.T. is funded by the John Templeton Foundation, and M.R.-G. had funding from an ICGC fellowship at the University of Minnesota. This work was supported by National Science Foundation grant DEB-1051115. We have no conflicting interests to declare.

Literature Cited

Bachmann, H. 2013. Availability of public goods shapes the evolution of competing metabolic strategies. Proceedings of the National Academy of Sciences of the USA 110:14302–14307.

Bell, G., and A. O. Mooers. 1997. Size and complexity among multicellular organisms. Biological Journal of the Linnean Society 60:345–363.

Bonner, J. T. 1998. The origins of multicellularity. Integrative Biology 1:27–36.

Bryan, A. K., A. Goranov, A. Amon, and S. R. Manalis. 2010. Measurement of mass, density, and volume during the cell cycle of yeast. Proceedings of the National Academy of Sciences of the USA 107: 999–1004.

Buss, L. W. 1987. The evolution of individuality. Princeton University Press, Princeton, NJ.

Chacón, J. M., W. Möbius, and W. R. Harcombe. 2018. The spatial and metabolic basis of colony size variation. ISME Journal 12:669–680.

Chao, L., and B. Levin. 1981. Structured habitats and the evolution of anticompetitor toxins in bacteria. Proceedings of the National Academy of Sciences of the USA 78:6324–6328.

Driscoll, W. W., and J. W. Pepper. 2010. Theory for the evolution of diffusible external goods. Evolution 64:2682–2687.

Escalante, A. E., M. Rebolleda-Gómez, M. Benitez, and M. Travisano. 2015. Ecological perspectives on synthetic biology: insights from microbial population biology. Frontiers in Microbiology 6:143.

Graham, L. E. 1993. Origin of land plants. Wiley, New York.

Greig, D., and M. Travisano. 2008. Density-dependent effects on allelopathic interactions in yeast. Evolution 62:521–527.

Grosberg, R. K., and R. R. Strathmann. 2007. The evolution of multicellularity: a minor major transition? Annual Review of Ecology, Evolution, and Systematics 38:621–654.

Hanski, I., M. Saastamoinen, and O. Ovaskainen. 2006. Dispersal-related life-history trade-offs in a butterfly metapopulation. Journal of Animal Ecology 75:91–100.

Harcombe, W. 2010. Novel cooperation experimentally evolved between species. Evolution 64:2166–2172.

Harcombe, W., W. J. Riehl, I. Dukovski, B. R. Granger, A. Betts, A. H. Lang, G. Bonilla, et al. 2014. Metabolic resource allocation in individual microbes determines ecosystem interactions and spatial dynamics. Cell Reports 7:1104–1115.

Herron, M. D., and R. E. Michod. 2008. Evolution of complexity in the volvocine algae: transitions in individuality through Darwin's eye. Evolution 62:436–451.

Koschwanez, J. H., K. R. Foster, and A. W. Murray. 2011. Sucrose utilization in budding yeast as a model for the origin of undifferentiated multicellularity. PLoS Biology 9:e1001122.

Lenski, R. E., M. R. Rose, S. C. Simpson, and S. Tadler. 1991. Long-term experimental evolution in *Escherichia coli*. I. Adaptation and divergence during 2,000 generations. American Naturalist 138:1315–1341.

Libby, E., and W. C. Ratcliff. 2014. Ratcheting the evolution of multicellularity. Science 346:426–427.

Libby, E., W. C. Ratcliff, M. Travisano, and B. Kerr. 2014. Geometry shapes evolution of early multicellularity. PLoS Computational Biology 10:e1003803.

Maynard Smith, J., and E. Szathmáry. 1995. The major transitions in evolution. Oxford University Press, Oxford.

Michod, R. E. 2007. Evolution of individuality during the transition from unicellular to multicellular life. Proceedings of the National Academy of Sciences of the USA 104(suppl.):8613–8618.

Michod, R. E., and D. Roze. 2001. Cooperation and conflict in the evolution of multicellularity. Heredity 86:1–7.

Mitri, S., J. B. Xavier, and K. R. Foster. 2011. Social evolution in multispecies biofilms. Proceedings of the National Academy of Sciences of the USA 108:10839–10846.

Monod, J. 1949. The growth of bacterial cultures. Annual Reviews of Microbiology 3:371–394.

Murdoch, D., and E. D. Chow. 2013. ellipse: functions for drawing ellipses and ellipse-like confidence regions. R package version 0.3-8. R Foundation for Statistical Computing, Vienna.

Okasha, S. 2005. Multilevel selection and the major transitions in evolution. Philosophy of Science 72:1013–1025.

Payne, J. L., A. G. Boyer, J. H. Brown, S. Finnegan, M. Kowalewski, R. Krause, S. K. Lyons, et al. 2009. Two-phase increase in the maximum size of life over 3.5 billion years reflects biological innovation and environmental opportunity. Proceedings of the National Academy of Sciences of the USA 106:24–27.

Pfeiffer, T., S. Schuster, and S. Bonhoeffer. 2001. Cooperation and competition in the evolution of ATP-producing pathways. Science 292:504–507.

Pinheiro, J., and D. Bates. 2000. Mixed-effects models in S and S-PLUS. Springer, New York.

Pinheiro, J., D. Bates, S. DebRoy, D. Sarkar, and R Development Core Team. 2015. nlme: linear and nonlinear mixed effects models. R Foundation for Statistical Computing, Vienna.

Platt, T. G., and J. D. Bever. 2009. Kin competition and the evolution of cooperation. Trends in Ecology and Evolution 24:370–377.

Queller, D. C. 1994. Genetic relatedness in viscous populations. Evolutionary Ecology 8:70–73.

Ratcliff, W. C., R. F. Denison, M. Borrello, and M. Travisano. 2012. Experimental evolution of multicellularity. Proceedings of the National Academy of Sciences of the USA 109:1595–1600.

Ratcliff, W. C., J. D. Fankhauser, D. W. Rogers, D. Greig, and M. Travisano. 2015. Origins of multicellular evolvability in snowflake yeast. Nature Communications 6:6102.

R Development Core Team. 2018. R: a language and environment for statistical computing. R Foundation for Statistical Computing, Vienna.

Rebolleda-Gómez, M., W. C. Ratcliff, and M. Travisano. 2012. Adaptation and divergence during experimental evolution of multicellular *Saccharomyces cerevisiae*. Pages 99–104 *in* C. Adami, D. M. Bryson, C. Ofria, and R. T. Pennock, eds. Artificial life. Vol. 18. MIT Press, Cambridge, MA.

Rebolleda-Gómez, M., and M. Travisano. 2018. Data from: The cost of being big: local competition, importance of dispersal, and experimental evolution of reversal to unicellularity. American Naturalist, Dryad Digital Repository, https://doi.org/10.5061/dryad.32b87rn.

Ritz, C., and J. C. Streibig. 2008. Nonlinear regression with R. Springer, New York.

Saxer, G., M. Doebeli, and M. Travisano. 2009. Spatial structure leads to ecological breakdown and loss of diversity. Proceedings of the Royal Society B 1664:2065–2067.

Schindelin, J., C. T. Rueden, M. C. Hiner, and K. W. Eliceiri. 2015. The ImageJ ecosystem: an open platform for biomedical image analysis. Molecular Reproduction and Development 82:518–529.

Sebé-Pedrós, A., B. M. Degnan, and I. Ruiz-Trillo. 2017. The origin of Metazoa: a unicellular perspective. Nature Review Genetics 18:498–512.

Smith, J., D. C. Queller, and J. Strassmann. 2014. Fruiting bodies of the social amoeba *Dictyostelium discoideum* increase spore transport by *Drosophila*. BMC Evolutionary Biology 14:105.

Sober, E., and D. S. Wilson. 1998. Unto others: the evolution and psychology of unselfish behavior. Harvard University Press, Cambridge, MA.

Solari, C. A., S. Ganguly, J. O. Kessler, R. E. Michod, and R. E. Goldstein. 2006. Multicellularity and the functional interdependence of motility and molecular transport. Proceedings of the National Academy of Sciences of the USA 103:1353–1358.

Sommer, U., E. Charalampous, S. Genitsaris, and M. Moustaka-Gouni. 2017. Benefits, costs and taxonomic distribution of marine phytoplankton body size. Journal of Plankton Research 39:494–508.

Stanley, S. M. 1973. An ecological theory for the sudden origin of multicellular life in the late Precambrian. Proceedings of the National Academy of Sciences of the USA 70:1486–1489.

Stearns, S. C. 1989. Trade-offs in life-history evolution. Functional Ecology 3:259–268.

Stewart, F. M., and B. R. Levin. 1973. Partitioning of resources and the outcome of interspecific competition: a model and some general considerations. American Naturalist 107:171–198.

Strassmann, J. E., Y. Zhu, and D. C. Queller. 2000. Altruism and social cheating in the social amoeba *Dictyostelium discoideum*. Nature 408:965–967.

Tarnita, C. E., C. H. Taubes, and M. A. Nowak. 2013. Evolutionary construction by staying together and coming together. Journal of Theoretical Biology 320:10–22.

Taylor, P. D. 1992. Altruism in viscous populations—an inclusive fitness model. Evolutionary Ecology 6:352–356.

Velicer, G. J., L. Kroos, and R. Lenski. 2000. A family of candidate taste receptors in human and mouse. Nature 404:598–601.

Vulin, C., J. Di Meglio, A. B. Linder, A. Daerr, A. Murray, and P. Hersen. 2014. Growing yeast into cylindrical colonies. Biophysical Journal 106:2214–2221.

West, S. A., R. M. Fisher, A. Gardner, and E. T. Kiers. 2015. Major evolutionary transitions in individuality. Proceedings of the National Academy of Sciences of the USA 112:10112–10119.

West, S. A., I. Pen, and A. S. Griffin. 2002. Cooperation and competition between relatives. Science 296:72–75.

Wilson, D. S., G. B. Pollock, and L. A. Dugatkin. 1992. Can altruism evolve in purely viscous populations? Evolutionary Ecology 6:331–341.

Yu, D. W., and H. B. Wilson. 2001. The competition-colonization trade-off is dead; long live the competition-colonization trade-off. American Naturalist 158:49–63.

Zor, T., and Z. Selinger. 1996. Linearization of the Bradford protein assay increases its sensitivity: theoretical and experimental studies. Analytical Biochemistry 236:302–308.

Associate Editor: Benjamin M. Bolker
Editor: Judith L. Bronstein

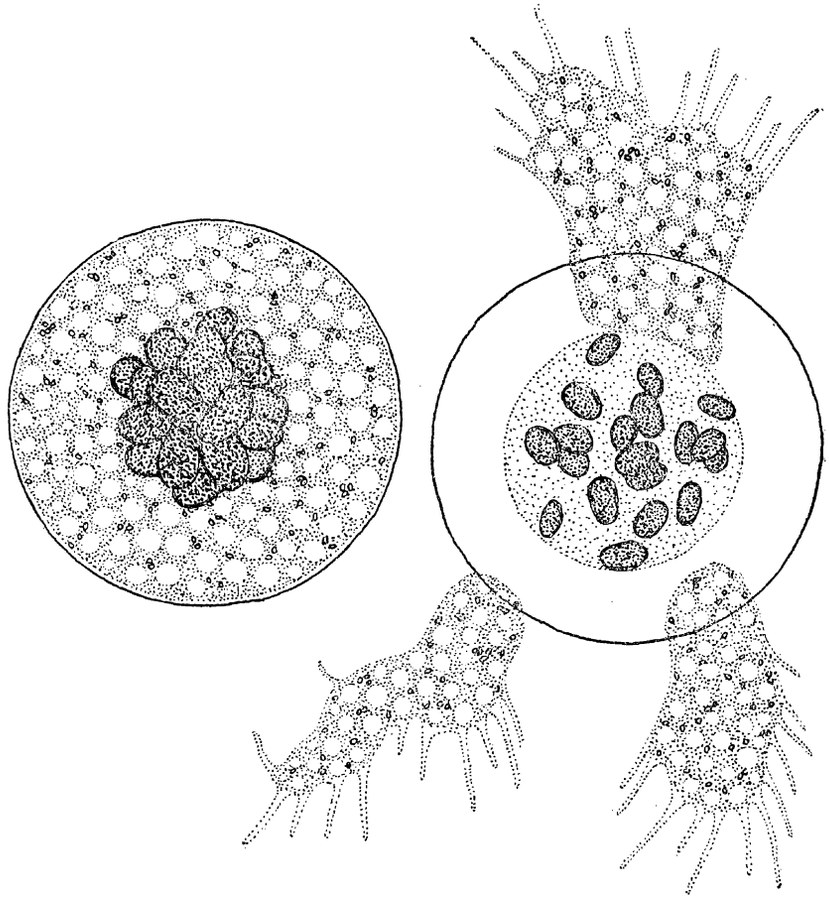

"Some time after the animal has gorged itself with food, or formed a central common vacuole of food, it withdraws its pseudopodia and enters into an encysted condition. . . . During the early part of the encystment the vacuoles are not conspicuous. As the end of the encysted condition approaches the vacuoles become more prominent. The cyst may rupture at one, two, three, or four places, and the contents escape through the clefts." From "Notes on the Genus *Leptophrys*" by William A. Kepner (*The American Naturalist*, 1906, 40:335–342).